January 01, 2010

Dependence of delay margin on network topology: single delay case

Wei Qiao
Northeastern University

Rifat Sipahi
Northeastern University

Dependence of Delay Margin on Network Topology: Single Delay Case

Wei Qiao * **Rifat Sipahi** *,1

* *Department of Mechanical and Industrial Engineering, Northeastern University, Boston, MA 02115 USA. (e-mail: qiao.w@husky.neu.edu, rifat@coe.neu.edu).*

Abstract: The main objective in this paper is to capture the indirect relationship between the delay margin τ^* of coupled systems and different graphs $\mathcal{G}$ these systems form via their different topologies, $\tau^* = \tau^*(\mathcal{G})$. A four-agent linear time invariant (LTI) consensus dynamics is taken as a benchmark problem with a single delay τ and second-order agent dynamics. In this problem, six possible topologies with graphs $\mathcal{G}_1, \ldots, \mathcal{G}_6$ exist without disconnecting an agent from all others. To achieve the objectives of the paper, we start with a recently introduced stability analysis technique called Advanced Clustering with Frequency Sweeping (ACFS) and reveal the delay margin τ^*, that is, the largest delay that the consensus dynamics can withstand without loosing stability. We next investigate how τ^* is affected as one graph transitions to another when some links between the agents weaken and eventually vanish. Finally, the damping effects to τ^* and the graph transitions are studied and discussed with comparisons. This line of research has been recently growing and new results along these lines promise delay-independent, robust and delay-tolerant topology design for coupled delayed dynamical systems.

Keywords: Stability, Topology, Delay margin, Delay Tolerant Network

1. INTRODUCTION

Studying the dynamics of coupled systems has impacts on multi-agent problems in formation control, flocking, distributed sensor networks, altitude alignment of clusters of satellites, mobile robots, unmanned air vehicles (UAVs), autonomous underwater vehicles (AUVs), automated highway systems and vehicular traffic follow, (Beard et al., 2006; Moreau and Ghent et al., 2004; Ren et al., 2005, 2007; Zou et al., 2007; Olfati-Saber, 2006; Olfati-Saber and Murray, 2004; Schollig et al., 2007; Munz et al., 2009). One of the crucial problems in these applications is the group agreement (consensus) which can be achieved with the awareness of the group members about the states of the other members combined with appropriate control laws. A well-known consensus problem arises, for instance, in follow-the-leader traffic flow, where each driver makes decisions to maintain a constant headway and to match the vehicle speed to that of the preceding vehicle, (Helbing, 2001; Orosz et al., 2005; Sipahi et al., 2007).

When multiple dynamics couple each other, the scale of the problem grows, but more importantly coupling pattern (network topology) also plays a role in determining the overall dynamic behavior (Helbing, 2001). This coupling pattern, that is, the network topology with graph $\mathcal{G}$ is the first focus in this paper. Often, when dynamics couple via a network, information sharing across the network becomes *delayed* due to many reasons, including the communication medium, network protocols, congestion in the communication lines, actuation and decision-making, (Loiseau et al., 2009). In such a scenario, instantaneous information is not available to the coupled dynamics (group members) due to delays τ. The presence of delays, which is a well-known source of instability, forms the second focus of this paper.

The problem studied in this paper is on the stability of coupled systems with $\mathcal{G}$ in the presence of delays in the communication lines among the systems. More specifically, we are interested in finding the maximum amount of delay τ^* that a particular network with graph $\mathcal{G}$ is tolerant without losing its stability. Delay τ^* is expected to be different for different $\mathcal{G}$, and we seek to reveal how τ^* relates to different network topologies $\tau^* = \tau^*(\mathcal{G})$. To demonstrate the results, linear time-invariant (LTI) four-agent consensus dynamics with a single delay is taken as a benchmark problem.

What is unique in this paper is that we explore the relationship between two indirectly related concepts; the network topology $\mathcal{G}$ and stability margin τ^*. There exist many studies that focus on addressing τ^* (Chen et al., 1995; Cooke and van den Driessche, 1986; Hale and Huang, 1993; Gu et al., 2005; Louisell, 2001; Michiels et al., 2007; Sipahi and Olgac, 2005; Stepan, 1989; Jarlebring, 2006), however only few work attempt to connect $\mathcal{G}$ and τ^* (Schollig et al., 2007; Sipahi and Acar, 2008). This article complements the existing work by considering higher order dynamics, homogeneous as well as heterogeneous agents, damping effects, and topology transitions. We study these on a LTI four-agent consensus problem, which can exhibit six different topologies $\mathcal{G}_1, \ldots, \mathcal{G}_6$ without disconnecting any agent from all the remaining ones. We then visit Advanced Clustering with Frequency Sweeping methodology (ACFS), (Delice and Sipahi, 2010), and reveal the τ^* for each $\mathcal{G}$. Next, we study the effects of damping to τ^* and report the results with comparisons. Based on the results, we also interpret how τ^* is affected as one transitions from one graph to another. To our best knowledge, we report for the first time the con-

[1] This research has been supported in part by the award from the National Science Foundation ECCS 0901442 and Dr. R. Sipahis start-up funds available at Northeastern University.

nections between different topologies, their transitions, agent heterogeneity, damping effects and τ^*.

The text is organized as follows. We first present the preliminaries related to mathematical modeling of coupled dynamics with delays and an overview of ACSF's algorithmic construct. Next, the stability analysis and arising results are presented. Future research directions and conclusions end the paper.

Notations are standard. We use $\mathbb{C}_+$, $\mathbb{C}_-$, $j\mathbb{R}$ for right half, left half and the imaginary axis of the complex plane, respectively. $\mathbb{R}$ represents the set of real numbers and j is the complex number. Matrices, vectors and sets are denoted by bold face, while the scalar entities are with normal font. The vector $\mathbf{v} \in \mathbb{R}_+^L$ defines an L-dimensional vector with positive real entries.

2. PRELIMINARIES

2.1 Linear Time Invariant Model With Delays

Let the state of agent k be denoted by $x_k(t)$. A commonly studied continuous-time LTI consensus dynamics is given by

$$\ddot{x}_k(t) = \sum_{\mu=1,\mu\neq k}^{4} \alpha_{\mu k} \left(x_\mu(t-\tau) - x_k(t)\right) - \beta \dot{x}_k(t), \quad (1)$$

where $k = 1 \dots 4$, $\tau > 0$ is the delay, the summation term is the controller with $\alpha_{\mu k} \in \mathbb{R}_+$, and μ is the subscript representing the agents sharing their state information with agent k based on the topology ($\mathcal{G}$) that determines which $\alpha_{\mu k}$ is zero or non-zero. Eq.(1) represents the dynamics of four agents, where $\beta \neq 0$ represents the damping effects, and each agent is aware of its state instantaneously, but only delayed states of the agents it is connected with.

It is straightforward to re-write Eq. (1) in matrix form as

$$\ddot{\boldsymbol{x}}(t) = \mathbf{A}\boldsymbol{x}(t) + \mathbf{B}\boldsymbol{x}(t)(t-\tau) + \mathbf{C}\dot{\boldsymbol{x}}(t), \quad (2)$$

where $\boldsymbol{x}(t) = (\boldsymbol{x}_1(t)..., \boldsymbol{x}_n(t))^T \in \mathbb{R}^{4\times 1}$ is the state vector, $n = 4$ is the number of states, and $\mathbf{A}, \mathbf{B}, \mathbf{C} \in \mathbb{R}^{4\times 4}$ are matrices with constant real entries. If the states of the agents converge to each other as time elapses, synchronization of the states is said to be achieved. This means that all the states agree with each other, that is, $\|x_\mu(t) - x_k(t)\| \to 0$, $\mu \neq k$ as $t \to \infty$ and (Ren et al., 2005; Olfati-Saber and Murray, 2004), or in other words, the error dynamics $x_\mu - x_j$ is asymptotically stable.

The delay differential equation (1) is not new, and has been studied extensively in various forms including string stability in vehicular traffic flow, time-variant effects, switching topology, single delay case and topology dependency (Ren et al., 2005; Olfati-Saber and Murray, 2004, 2003a,b; Schollig et al., 2007; Sipahi et al., 2007; Bose and Ioannou, 2003; Orosz et al., 2005). On the other hand, the non-conservative stability features of (2) in connection with $\mathcal{G}$ are open problems.

Remark 1. Note that the system in Eq. (2) has an invariant pole $s = 0$ in $\mathbb{C}$ for any delay τ. As we confirmed, this pole, which creates the rigid body dynamics of the agents, does not invite any additional $s = 0$ poles for some $\tau \geq 0$, and thus it does not play any role on the stability of (2) for $\tau > 0$. Consequently, we focus only on the stability of the remaining dynamic modes of (2). If these modes are asymptotically stable, then we call Eq.(2) asymptotically stable disregarding the rigid body dynamics.

2.2 Stability Analysis

The characteristic equation of (2) is given by

$$f(s, \tau, \alpha_{\mu k}) = \det[s^2\,\mathbf{I} - \mathbf{A} - \mathbf{B}\,e^{-\tau s} - s\,\mathbf{C}] = 0, \quad (3)$$

where $s \in \mathbb{C}$ is the Laplace variable and $\mathbf{I}$ is the identity matrix. In order to study the asymptotic stability of Eq. (2) with respect $\alpha_{\mu k}$ and τ, one needs to investigate the locations of the roots of Eq. (3), s, on the complex plane $\mathbb{C}$. As per stability condition, for any given τ and $\alpha_{\mu k}$, dynamics in Eq. (2) is asymptotically stable if and only if all the infinitely many roots of Eq. (3) are in $\mathbb{C}_-$, (Cooke and van den Driessche, 1986; Stepan, 1989). Clearly, checking the stability condition in the entire s domain is a prohibitively difficult task.

In this study, we deploy Advanced Clustering with Frequency Sweeping methodology (ACFS) (Delice and Sipahi, 2010) in order to solve for the delay margin τ^*, that is, the largest delay value that the system in (2) can withstand without loosing stability. It is proven earlier that the stability of TDS that (2) is a subclass of may change only when (2) has eigenvalues on the imaginary axis, that is, when $f(j\omega, \tau, \alpha_{\mu k}) = 0$ (Datko, 1978). Similar to many other methods, ACFS also exploits this knowledge to extract the stability characteristics of delay systems, as we review next.

2.3 Review of ACFS

ACFS starts similar to the CTCR methodology (Sipahi and Olgac, 2005), but ACFS can also handle stability analysis of systems with more than three delays (Delice and Sipahi, 2010). For single delay problems, as it is the case here, ACFS is implemented as follows. Replace the exponential function in (3) with the substitution,

$$e^{-\tau s} = \frac{1 - Ts}{1 + Ts},\ T \in \mathbb{R},\ s = j\omega \in j\mathbb{R}, \quad (4)$$

where

$$\tau = \frac{2}{\omega}[\arctan(\omega T) \pm \ell\pi], \quad \ell = 0, 1, 2, \dots, \quad (5)$$

with $0 \leq \arctan(\cdot) < \pi$. Substitution of (4) into (3), after some manipulations, leads to a new polynomial,

$$g(s, T, \alpha_{\mu k}) = \sum_{\ell=0}^{3n} Q(s, \alpha_{\mu k}) T^\ell = 0. \quad (6)$$

It was proven in (Sipahi and Olgac, 2005) that $s = j\omega$ solutions of $f(s, \tau, \alpha_{\mu k}) = 0$ and $g(s, T, \alpha_{\mu k}) = 0$ are identical for some τ and T, respectively, where T and τ are interrelated via Eq. (5). This proof is central for ACFS, which connects the analysis of transcendental quasi-polynomials to algebraic polynomials via algebraic geometry.

ACFS starts with requiring that the following equations hold concurrently when Eq. (6) has a solution,

$$g_{\Re} = \Re[g(j\omega, T, \alpha_{\mu K})] = 0, \quad (7)$$

$$g_{\Im} = \Im[g(j\omega, T, \alpha_{\mu K})] = 0, \quad (8)$$

where

$$g_{\Im} = \sum_{i=0}^{c} b_i(\omega, \alpha_{\mu k})\, T^i = 0\,, \quad b_{c_2} \neq 0\,, \quad (9)$$

$$g_{\Re} = \sum_{i=0}^{c} a_i(\omega, \alpha_{\mu k})\, T^i = 0\,, \quad a_{c_2} \neq 0\,, \quad (10)$$

where all a_i's and b_i's are real polynomials with respect to ω, and $c > 0$ is the commensurate degree of τ in (3). In order to solve (9)-(10), T can be eliminated using the resultant theory, Collins (1971). This requires the construction of the Sylvester's matrix $\mathbf{S}$

$$\mathbf{S} = \begin{bmatrix} a_c & a_{c-1} & . & . & . & a_0 & 0 & 0 & 0 \\ 0 & a_c & a_{c-1} & . & . & a_1 & a_0 & 0 & 0 \\ . & . & . & . & . & . & . & . & . \\ . & . & . & . & . & . & a_1 & a_0 & \\ b_c & b_{c-1} & . & . & . & b_0 & 0 & 0 & 0 \\ 0 & b_c & b_{c-1} & . & . & b_1 & b_0 & 0 & 0 \\ . & . & . & . & . & . & . & . & . \\ . & . & . & . & . & . & b_1 & b_0 & \end{bmatrix}. \quad (11)$$

If (9)-(10) have a common root, then $\mathbf{S}$ is singular at the common roots. In other words, the singularity of $\mathbf{S}$ is a necessary condition for the equations in (9)-(10) to have common solutions. Given $\alpha_{\mu k}$, the singularity of $\mathbf{S}$ can be investigated by analyzing the single-variable polynomial

$$V(\omega) = \det(\mathbf{S}) = 0, \quad (12)$$

from which the candidate $\tilde{\omega} \in \mathbb{R}_+$ solutions can be computed. If common $(\tilde{\omega}, \tilde{T})$ solutions exist in (9)-(10), they can be easily found from these equations using $\tilde{\omega}$, and the corresponding infinitely many $\tilde{\tau}$ can be computed from Eq. (5).

In all the scenarios considered here, the delay-free problem ($\tau = 0$) is asymptotically stable (see Remark 1). Hence the identification of the delay margin τ^* can be done by choosing the smallest positive of the infinitely many $\tilde{\tau}$ solutions. All the delay values less than the delay margin τ^* guarantee that (2) is asymptotically stable.

3. NUMERICAL RESULTS

We consider a four-agent problem where each agent is a node and exhibits the dynamics defined in (1), and each node is coupled with undirected communication lines to some of the other nodes. The fully connected graph $\mathcal{G}_1$ is the topology we start with (Figure 1), where each link between the nodes are represented by a coupling strength $\alpha_{\mu k}$ (or a controller gain) and a communication delay τ.

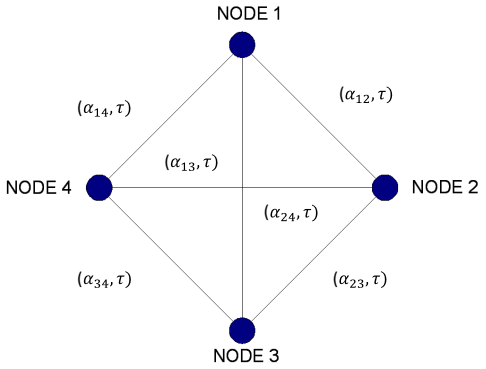

Fig. 1. Four-agents forming six undirected links.

Notice that six different topologies with graphs $\mathcal{G}_p$, $p = 1, \ldots, 6$ arise by connecting the four nodes in Figure 1 in different ways, without disconnecting a node from all others, Figure 2. We now quest what the delay margin τ^* is for each one of the topologies. This can be done by setting some of the $\alpha_{\mu k}$ coupling strengths to zero accordingly. The following subsections discuss the dependency of stability on different graphs $\mathcal{G}_p$ with homogeneous or heterogeneous coupling strengths, stability transitions between topology configurations, and the effects of damping constant β on the stability margin τ^*.

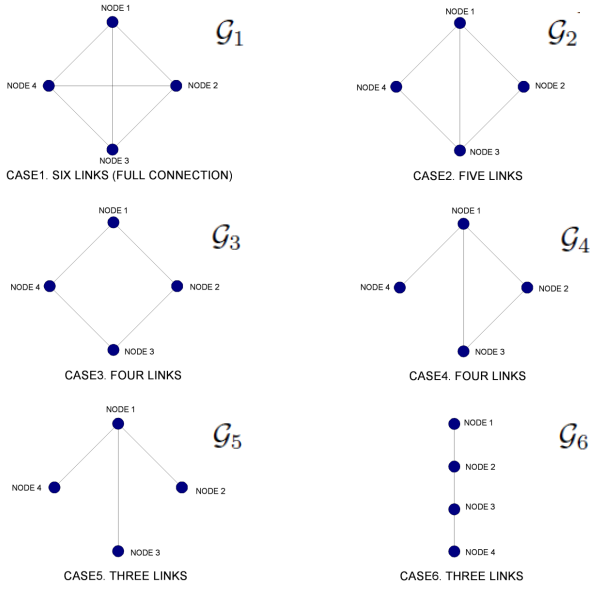

Fig. 2. Six different configurations of topology.

3.1 *Dependence of Delay Margin on Topology - Weak Damping Case*

In order to reveal the relationship between τ and $\mathcal{G}$ without the interference of other parameters, we assume that agents have identical coupling strengths, $\alpha_{\mu k} = \alpha$, and $\beta = 0.01$. For the graph $\mathcal{G}_1$ in Figure 1, the system matrices in (2) are given by

$$\mathbf{A} = -3\alpha\mathbf{I}, \ \mathbf{B} = \alpha(\mathbf{1} - \mathbf{I}), \ \mathbf{C} = -\beta\mathbf{I},$$

with compatible dimensions, where $\mathbf{1}$ is a matrix with all its entries unity. Matrices corresponding to other graphs can be similarly obtained and thus suppressed.

We next implement ACFS and compute τ^* for $\alpha = 1$ for each topology in Figure 2. The results are shown in Figure 3. Inspecting Figure 3 results that the fully connected $\mathcal{G}_1$ exhibits the largest delay margin among all. Interestingly, $\mathcal{G}_3$ with four links has smaller τ^* than $\mathcal{G}_6$ that has three links. This indicates that a network with missing connections does not always mean that the dynamics it couples will exhibit smaller τ^*, but in the contrary, in some cases, the topology induces larger stability margins by losing a connection. This observation is valid for both the transitions $\mathcal{G}_2 \rightarrow \mathcal{G}_4$ and $\mathcal{G}_3 \rightarrow \mathcal{G}_6$. Below, we will explore this observation further.

3.2 *Effects of Topology Transition on Stability*

Stability Transition when $\mathcal{G}_2 \rightarrow \mathcal{G}_4$: Discovered from Figure 3, the topology transition from $\mathcal{G}_2$ to $\mathcal{G}_4$ leads to larger stability margin. The coupling strength α_{34} is responsible for this transition, and we investigate its effects to the stability margin by deploying the ACFS, see Figure 4 for results. Notice in Figure 4 that the change of τ^* at $\alpha_{34} = 1$ reveals significantly high sensitivity with respect to α_{34}. In Figure 5, we present this sensitivity as α_{34} changes from zero to two. Furthermore, we notice that transition from $\mathcal{G}_2$ to $\mathcal{G}_4$ (by losing one connection) enhances stability margin, contrary to the transition from $\mathcal{G}_1$ to

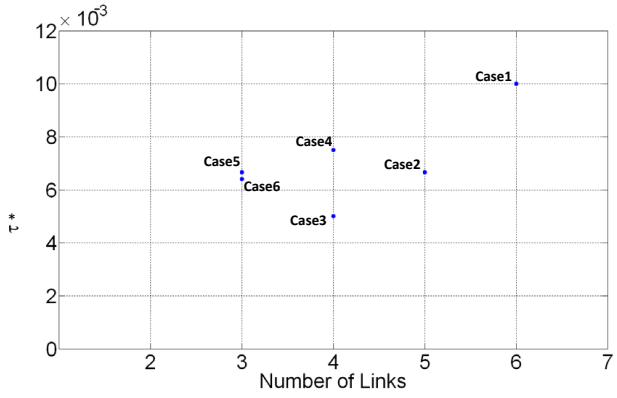

Fig. 3. Delay margin τ^* with respect to Case p for topology graph $\mathcal{G}_p$ in Figure 2. $\alpha = 1$ and $\beta = 0.01$.

$\mathcal{G}_2$. In both transitions, we reveal significantly high sensitivity in τ^* when the responsible coupling strength becomes unity, see Figure 5 and Figure 7.

Stability Transition when $\mathcal{G}_3 \rightarrow \mathcal{G}_6$: Topology transition from $\mathcal{G}_3$ to $\mathcal{G}_6$ while losing one link also improves τ^*. By deploying ACFS, the stability margin is captured as α_{14} sweeps from 0 to 2, see Figure 6. Similar to the transition from $\mathcal{G}_2$ to $\mathcal{G}_4$, losing one link yields larger τ^* and ultimately larger stable regions. Different from $\mathcal{G}_2 \rightarrow \mathcal{G}_4$ transition, we do not observe any high sensitivity with respect to the responsible coupling strength α_{14}, and the system monotonically loses stability region as α_{14} increases from zero to two.

Stability Transition when $\mathcal{G}_1 \rightarrow \mathcal{G}_2$: The transition from $\mathcal{G}_1$ to $\mathcal{G}_2$ occurs when α_{24} sweeps from $\alpha_{24} = 1$ to $\alpha_{24} = 0$, see Figure 2. The stability margin during this transition is shown in Figure 7. In Figure 7, as α_{24} approaches unity (thus graph $\mathcal{G}_1$ is recovered), τ^* becomes sensitive to changes in α_{24}, and a small change in α_{24} could result in a significant change of the shaded stability region. This interesting feature also occurs in the transition from $\mathcal{G}_2$ to $\mathcal{G}_4$ as α_{34} approaches unity, see Figure 4.

3.3 Stability Margin with Random Coupling Strengths

We next study the system with the topology $\mathcal{G}_1$ for the case when we randomly pick the six coupling strengths $\alpha_{\mu k}$ from a uniform distribution with $\alpha_{\mu k}$ being between zero and one. We

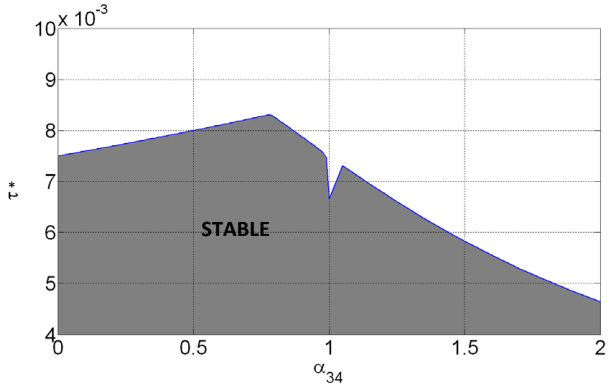

Fig. 4. Delay margin τ^* with respect to α_{34} in $\mathcal{G}_2$. Shaded region corresponds to stable dynamics. $\beta = 0.01$.

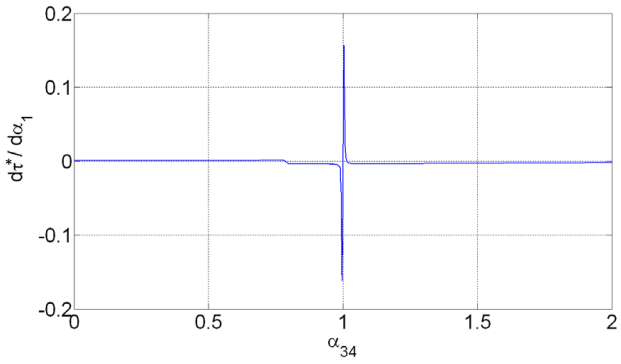

Fig. 5. Sensitivity variation as α_{34} sweeps from 0 to 2.

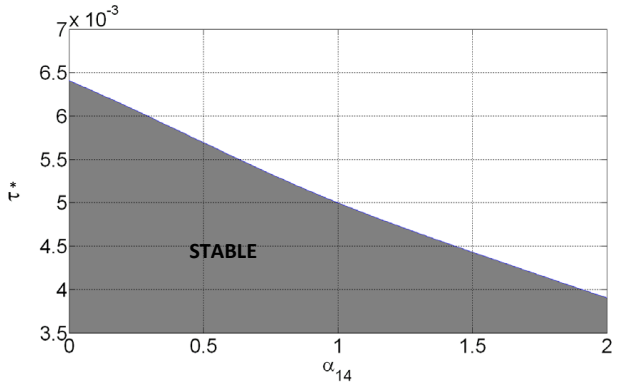

Fig. 6. Delay margin τ^* with respect to α_{14} in $\mathcal{G}_3$. Shaded region corresponds to stable dynamics. $\beta = 0.01$.

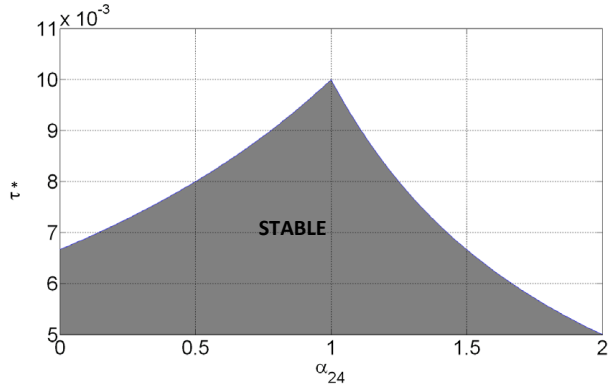

Fig. 7. Delay margin τ^* with respect to α_{24} in $\mathcal{G}_1$. Shaded region corresponds to stable dynamics. $\beta = 0.01$.

perform the stability analysis with 20 trials, where in each trial we randomize the six coupling strengths in MATLAB seeded with the computer clock. In all the cases in the stability analysis, damping is fixed at $\beta = 0.01$. As expected, in each trial, a different delay margin τ^* is found, see Figure 8. Although this figure may not be conclusive, 20 trials still give a certain degree of confidence on the results. Interestingly, the minimum of τ^* in Figure 8 matches with the delay margin of the same problem when $\alpha_{\mu k} = 1$, see Figure 3 - Case 1. Further research along these lines are left for future work.

3.4 Stability Analysis with Respect to Damping

In the previous sections, damping constant is chosen as $\beta = 0.01$. In this section, the effects of β to τ^* are inspected by

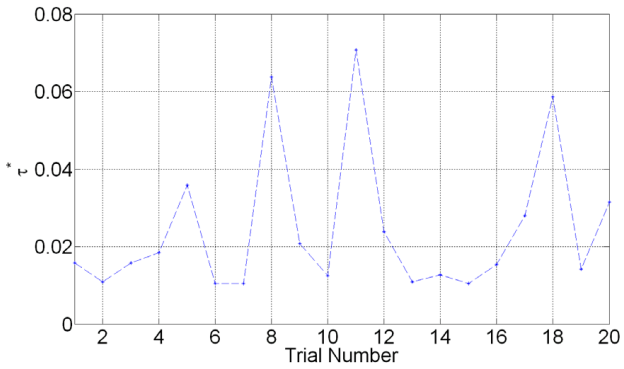

Fig. 8. Stability margin of the system with the topology $\mathcal{G}_1$ for 20 different trials, where in each trial all the six coupling strengths $\alpha_{\mu k}$ are randomized from a uniform distribution with $\alpha_{\mu k}$ being between zero and one, and where each randomization is seeded with the computer clock.

choosing β as 0.1, 0.2, 0.3. We then repeat the same analysis as in the previous section to investigate the damping effects.

Damping effects to transition in $\mathcal{G}_2$: Figure 9 shows the transition of $\mathcal{G}_2$ with respect to α_{34} for different β values. It reveals that sensitivity around $\alpha_{34} \approx 1$ is decreasing as β gets larger (Figure 10). Moreover, we see that stable region below the respective curves enlarges as β increases, and the singularity point remains around $\alpha_{34} \approx 0.78$.

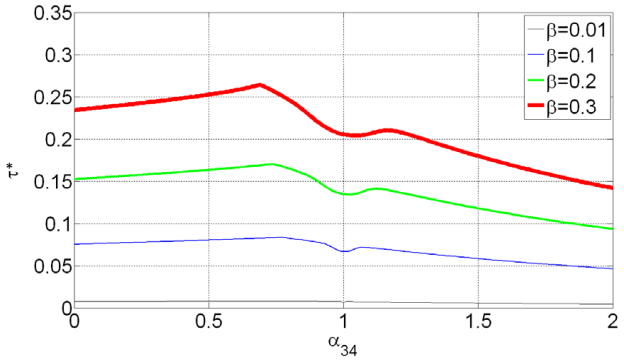

Fig. 9. Damping effect to delay margin as α_{34} changes in $\mathcal{G}_2$.

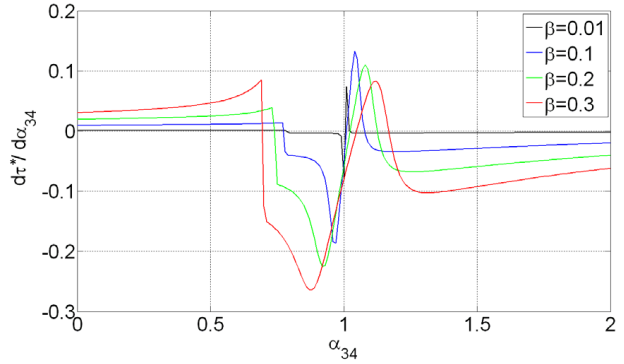

Fig. 10. Damping effect to sensitivity of delay margin as α_{34} changes in $\mathcal{G}_2$.

Damping effects in $\mathcal{G}_1$ and $\mathcal{G}_3$: Similar to $\mathcal{G}_2$, stable region enlarges with increasing β in $\mathcal{G}_1$ and $\mathcal{G}_3$, see Figure 12 and Figure 11, respectively.

Remark 2. In many examples in the literature (Stepan, 1989), it is shown that damping enhances the stability and enlarges the stability regions in delay parameter space. For the three specific topologies investigated here, we have revealed similar results that damping increases the delay margin. We finally note that the stability analysis results presented in this article are also confirmed by CTCR method (Sipahi and Olgac, 2006) and TRACE-DDE software (Breda et al., 2006). Other stability analysis methods for single delay systems can be found in (Chen and Latchman, 1995; Chen et al., 1995; Cooke and van den Driessche, 1986; Louisell, 2001; Stepan, 1989).

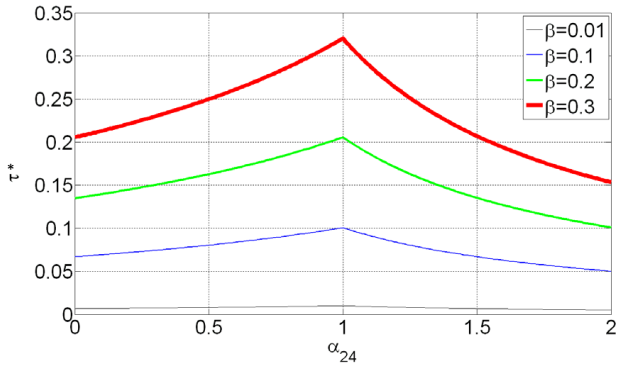

Fig. 11. Damping effect to transition with respect to α_{24} in $\mathcal{G}_1$.

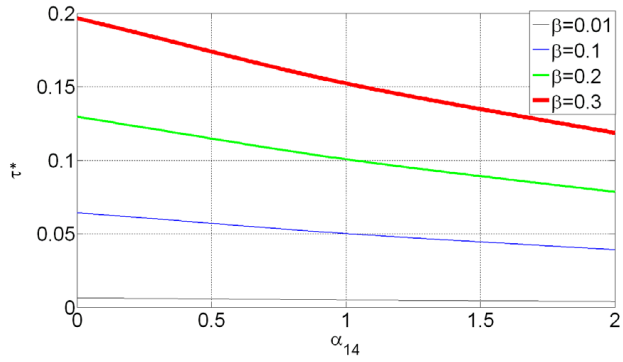

Fig. 12. Damping effects to delay margin as α_{14} changes in $\mathcal{G}_3$.

4. CONCLUSION

The effects of different topologies of coupled systems to the largest delay, that is, the delay margin τ^*, these systems can withstand is studied via a new technique called Advanced Clustering with Frequency Sweeping (ACFS). We present the results on a linear time-invariant four-agent consensus dynamics in which homogeneous or heterogeneous agents become aware of each other's states only after a delay τ. Some expected results arise from the analysis, such as fully connected graph considered renders the largest τ^* and increased damping in the system enhances τ^*. On the other hand, some counter-intuitive results are also captured. The most interesting one is that, in some cases, topologies with less number of links among the agents have larger delay margins compared to topologies with more links. We find that this claim holds true even when a topology transits to another while a responsible link weakens and eventually vanishes. We finally note that the stability margin of some topologies become extremely sensitive with respect to the coupling strengths of some links between the agents. Future

work along these lines include the consideration of larger scale problems with multiple delays, as well as the design of delay-independent topologies using algebraic tools.

REFERENCES

Beard, W.B., McLain, T.W, Nelson, D.B., Kingston, D., Johanson D. (2006). Decentralized Cooperative Aerial Surveillance Using Fixed-Wing Miniature UAVs. *Proc. IEEE*, 94(7), 1306-1324.

Bose, A., Ioannou, P. A. (2003). Analysis of Traffic Flow with Mixed Manual and Semiautomated Vehicles. *IEEE Tran. Intell. Transp. Sys.*, 4(4), 173-188.

Breda, D., Maset, S., and Vermiglio, R. (2006). Pseudospectral Differencing Methods for Characteristic Roots of Delay Differential Equations. *SIAM Journal of Scientific Computing*, 27, 482-495.

Chen, J. and Latchman, H. A. (1995). Frequency sweeping tests for asymptotic stability independent of delay. *IEEE Transactions on Automatic Control*, 40(9), 1640-1645.

Chen, J., Gu, G. and Nett, C. N. (1995). A new method for computing delay margins for stability of linear delay systems. *Systems and Control Letters*, 26(2), 107-117.

Cooke, K. L. and van den Driessche, P. (1986). On zeros of some transcendental equations. *Funkcialaj Ekvacioj*, 29(1), 7790.

Collins, G. E. (1971). The calculation of multivariate polynomial resultants. *Journal of the Association for Computing Machinery*, 18(4), 515532.

Datko, R. (1978). A procedure for determination of the exponential stability of certain differential-difference equations. *Quart. Appl. Math.*, 36, 279-292.

Delice, I.I., Sipahi, R. (2010). Advanced Clustering with Frequency Sweeping(ACFS) Methodology for the Stability. *Analysisof Multiple Time Delay Systems*. submitted to IEEE Transactions on Automatic Control, and to be presented at American Control Conference, Baltimore, MD.

Gu, K., Niculescu, S.I., Chen, J. (2005). On Stability Crossing Curves for General Systems with Two Delays. *J. Math. Anal. Appl.*, 311, 231-253.

Hale, J. K., Huang, W. (1993). Global Geometry of the Stable Regions for Two Delay Differential Equations. *Journal of Mathematical Analysis and Applications*, 178, 344-362.

Helbing, D. (2001). Traffic and Related Self-Driven Many-Particle Systems. *Rev. Mod. Phy.*, 73, 1067-1141.

Jarlebring, E. (2006). Computing the Stability Region in Delay-Space of a TDS Using Polynomial Eigenproblems. *6th IFAC Workshop on Time-Delay Systems*, L'Aquila, Italy.

Louisell, J. (2001). A matrix method for determining the imaginary axis eigenvalues of a delay system. *IEEE Transactions on Automatic Control*, 46(12), 2008-2012.

Loiseau, J.J., Michiels, W., Niculescu, S.-I., Sipahi, R. (2009). Topics in Time Delay Systems Analysis, Algorithms and Control. *Springer-Verlag*.

Michiels, W., Niculescu, S.I. (2007). Stability and Stabilization of Time-Delay Systems: An Eigenvalue-Based Approach. *SIAM Advances in Design and Control*, 12, Philadelphia.

Moreau, L., Ghent, S. (2004). Stability of Continuous-Time Distributed Consensus Algorithms. *43rd IEEE Conference on Decision and Control, Atlantis*, Paradise Island, Bahamas.

Munz, U., Papachristodoulou, A. and Allgwer, F. (2009). Consensus Reaching in Multi-Agent Packet-Switched Networks with Nonlinear Coupling. *International Journal of Control*, 82(5), 953-969.

Olfati-Saber, R. (2006). Flocking for Multi-Agent Dynamic Systems: Algorithms and Theory. *IEEE Trans. Aut. Cont.*, 51(3), 401-420.

Olfati-Saber, R., Murray, R.M. (2004). Consensus Problems in Networks of Agents with Switching Topology and Time-Delays. *IEEE Trans. Aut. Cont.*, 49(9), 1520-1533.

Olfati-Saber, R., Murray, R.M. (2003a). Consensus Protocols for Networks of Dynamic Agents. *American Control Conference*, Denver, Colarado.

Olfati-Saber, R., Murray, R. M. (2003b). Agreement Problems in Networks with Directed Graphs and Switching Topology. *Conference on Decision and Control*, Maui, Hawaii.

Orosz, G., Krauskopf, B. Wilson, R.E. (2005). Bifurcations and multiple traffic jams in a car-following model with reaction time delay. *Phys. D*, 211, 277-293.

Ren, W., Beard, R.W., Atkins, E.M. (2005). A Survey of Consensus Problems in Multi-agent Coordination. *American Control Conference*, Portland, OR.

Ren, W., Moore, K.L., Chen, Y. (2007). High-order and Model Reference Consensus Algorithms in Cooperative Control of MultiVehicle Systems. *ASME J. Dyn.Sys., Meas. Cont.*, 129, 678-688.

Schollig, A., Munz, U., Allgower, F. (2007). Topology-Dependent Stability of a Network of Dynamical Systems with Communication Delays. *Proceedings of the European Control Conference*, Kos, Greece.

Sipahi, R., Acar, A. (2008). Stability Analysis of Three-Agent Consensus Dynamics with Fixed Topology and Three Non-Identical Delays. *ASME Dynamic Systems and Control Conference*, Ann Arbor, Michigan, October.

Sipahi, R., Olgac, N. (2006). A Comparison of Methods Solving the Imaginary Characteristic Roots of LTI Time Delayed Systems. *SIAM J. Cont. Optim.*, 45(5), 1680-1696.

Sipahi, R., Niculescu, S.-I., Atay, F. (2007). Effects of Short-Term Memory of Drivers on Stability Interpretations of Traffic Flow Dynamics. *American Control Conference*, New York.

Sipahi, R., Olgac,N. (2005). Complete Stability Map of Third Order LTI, Multiple Time-Delay Systems. *Automatica*, 41(8), 1413-1422.

Stepan, G. (1989). Retarded Dynamical Systems: Stability and Characteristic Functions. *ser. Pitman Research Notes in Mathematics Series*, New York: Longman Scientific and Technical, co-publisher John Wiley and Sons, Inc., vol. 210.

Zou, Y., Pagilla, P.R., Misawa, E. (2007). Formation of a Group of Vehicles with Full Information Using Constraint Forces. *ASME J. Dyn.Sys., Meas. Cont.*, 129, 654-661.